

New Method of Determining Contact Angle between Monofilament and Liquid

JUN-ICHI YAMAKI and YUZO KATAYAMA, *Ibaraki Electrical
Communication Laboratory, Nippon Telegraph and Telephone Public
Corporation, Tokai-mura Naka-gun Ibaraki-ken, Japan*

Synopsis

This paper describes a method to obtain contact angle by observing the shape of a liquid drop attached to a monofilament. The relations between contact angle and the dimensions of drops are theoretically obtained. Thus, it is possible to calculate the contact angle if drop shape is measured. Through use of this method, the contact angles of epoxy resin on various kinds of monofilaments were measured. It was found that this method has practical utility for measurement of the contact angle between liquid and monofilament.

INTRODUCTION

With various advancements in fiber-reinforced plastic, contact angle of liquid on the monofilament has become important as the measure of wettability¹ between matrix polymer and monofilaments. If the wettability is not good, composites involve many voids, and so the shear strength of these composites decreases.^{2,3} In the case of very thin monofilaments, whose diameters are about 5 μ (for example, carbon fiber), it is very difficult to measure the contact angle directly by the usual method.^{2,3}

This paper describes a method by which contact angle of the monofilament can be obtained from liquid-drop-shape measurement.

First, the theory of a liquid drop attached to a monofilament is discussed. The drop shape attached to monofilament was derived by using Laplace's central field of force approach,⁴ and the relation between the contact angle and the drop size was obtained. Contact angles between epoxy resin and various kinds of monofilaments [fibers of carbon, polyethylene, poly(vinyl chloride), polycarbonate, acetal copolymer, nylon 6, and glass] have been measured by this method. The results explain the utility of this method.

BASIC THEORY

Drop Shape

If one regards a monofilament as a cylinder and neglects the effect of gravity, then the shape of a drop is symmetrical with respect to the x-axis, as

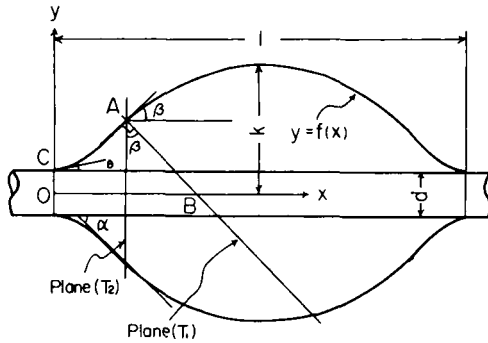


Fig. 1. Cross section of a drop and its parameters.

shown in Figure 1. Pressure difference between liquid phase and gas phase (ΔP) is given by eq. (1):⁴

$$\Delta P = \gamma_{LV} (1/R_1 + 1/R_2) \tag{1}$$

where γ_{LV} is the surface tension between liquid and gas, and $1/R_1$ and $1/R_2$ are normal curvatures of the surface whose curves on the surface are perpendicular to each other.

Rewrite R_1 and R_2 . Let $y, f(x)$ be the distance from drop surface to the x-axis. Then R_1 [radius of curvature of curve $y = f(x)$] is expressed as follows:

$$R_1 = - \left[1 + \left(\frac{dy}{dx} \right)^2 \right]^{3/2} / \frac{d^2y}{dx^2} \tag{2}$$

Next, R_2 is represented as a function of x and y . Let plane (T_1) include point A and be perpendicular to curve $y = f(x)$ at point A. And let plane (T_2) also include point A and be perpendicular to the x-axis. Let curve (a) be the intersection between drop surface and plane (T_1). Let curve (b) be the intersection between drop surface and plane (T_2). (Fig. 2).

Then, from the relation between R_1 and R_2 , R_2 is found to be included in plane (T_1) and to be the radius of curvature of curve (a) at point A. Consid-

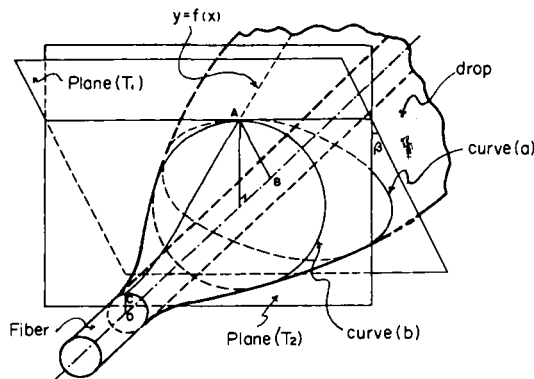


Fig. 2. Stereograph of a drop: Plane (T_1) includes point A and is perpendicular to curve $y = f(x)$. Plane (T_2) includes point A and is perpendicular to the x-axis. Curve (a) shows the intersection between drop surface and plane (T_1). Curve (b) is that of plane (T_2).

ering drop-surface symmetry with respect to the x-axis, curve (b) is a circle whose radius is y . The angle between plane (T_1) and plane (T_2) is β ($\tan \beta = dy/dx$): so, from Meusnier's theorem, R_2 is $y/\cos \beta$ and is expressed as follows:

$$R_2 = y[1 + (dy/dx)^2]^{1/2}. \tag{3}$$

From eqs. (1), (2), and (3), we find

$$\frac{d^2y}{dx^2} = -\frac{\Delta P}{\gamma_{LV}} \left[1 + \left(\frac{dy}{dx}\right)^2 \right]^{3/2} + \left[1 + \left(\frac{dy}{dx}\right)^2 \right] / y. \tag{4}$$

ΔP is constant through the drop, so we can solve eq. (4) if we regard $\Delta P/\gamma_{LV}$ as a constant. Then the shape of drops can be obtained as a function of $\Delta P/\gamma_{LV}$.

Because eq. (4) can not be solved analytically, it is changed into a difference equation and solved numerically through use of a computer. $y_0, [dy/dx]_{x=x_0}$, and x_0 at point C in Figure 1 are selected as the boundary conditions. y_0 is the radius of monofilament and $[dy/dx]_{x=x_0}$ is the tangent of contact angle ($\tan \theta$). Then the x-axis is divided into small spaces by Δx intervals. The divided points are $x_0, x_1, x_2, \dots, x_i, \dots$; and the corresponding y are $y_0, y_1, y_2, \dots, y_i, \dots$.

So we have

$$y_i = y_{i-1} + \left[\frac{dy}{dx} \right]_{x=x_{i-1}} \Delta x; \tag{5}$$

$$\left[\frac{dy}{dx} \right]_{x=x_i} = \left[\frac{dy}{dx} \right]_{x=x_{i-1}} + \left[\frac{d^2y}{dx^2} \right]_{x=x_{i-1}} \Delta x \tag{6}$$

$$(i = 1, 2, 3, 4, \dots).$$

From these boundary conditions and eqs. (4), (5), and (6), $y_1, y_2, \dots, y_i, \dots$ can be calculated.

Appearance of Similar Drops

Let us consider two monofilaments which are made of the same quality of material but whose diameters are different. Similar shapes of drops can be attached to these monofilaments.

Next, we explain why similar drops appear. We change the coordinate system (x, y) to (ξ, η) and define ξ, η by

$$x = n\xi \quad (n; \text{constant}) \tag{7}$$

$$y = n\eta. \tag{8}$$

Equation (4) with eqs. (7) and (8) may be rewritten as

$$\frac{d^2\eta}{d\xi^2} = -\frac{n\Delta P}{\gamma_{LV}} \left[1 + \left(\frac{d\eta}{d\xi}\right)^2 \right]^{3/2} + \left[1 + \left(\frac{d\eta}{d\xi}\right)^2 \right] / \eta. \tag{9}$$

If we replace η, ξ , and $n\Delta P$ in eq. (9) with y, x , and ΔP , respectively, eq. (9) reduces to eq. (4). This means that after all we can find a similar drop whose pressure difference (ΔP) is n times the original one when the diameter of a monofilament becomes one- n th.

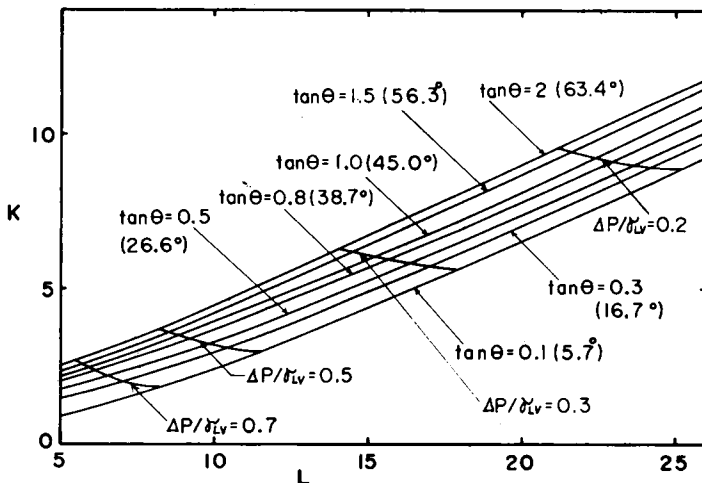


Fig. 3. Calculated relations between L and K under conditions of contact angles (θ) = 5.7° , 16.7° , 26.6° , 38.7° , 45.0° , 56.3° , and 63.4° .

This property of drop shape has a very important meaning when contact angle is measured, as will be explained in the following section.

CONTACT ANGLE

Direct measurement of the contact angle of a drop attached to a monofilament is very difficult, because the drop surface changes steeply near the point where the liquid surface is in contact with the monofilament.

Generally, drop surface is determined by eq. (4) if monofilament diameter (d), contact angle (θ), and ratio of pressure difference to surface tension ($\Delta P/\gamma_{LV}$) are given. This can also be done if the other three parameters are given. Then, the relations between parameters (d , θ , $\Delta P/\gamma_{LV}$) and the other three parameters (d , drop size) can be calculated by using eq. (4). Therefore, from these relations, contact angle can be found by measurement of d and drop size. As similar drop shapes appear even if the diameters of monofilaments are different, only the relations between (θ , $\Delta P/\gamma_{LV}$) and drop size are sought where monofilament radius is unity ($d = 2$).

Selection of drop-size parameters gives various measurement methods.

The L-, K-Method

Let l and k be drop length along the monofilament and maximum drop radius, respectively, as shown in Figure 1. If L and K are l and k where monofilament radius is unity, l and k can be translated into L and K , by using the following eqs. (10) and (11):

$$L = 2l/d; \quad (10)$$

$$K = 2k/d. \quad (11)$$

The relations between (L, K) and contact angles are shown in Figure 3. Calculation error was examined by changing Δx , which is a parameter indi-

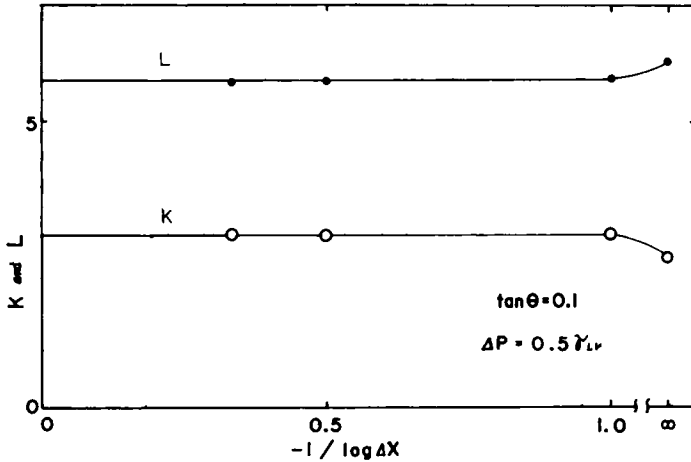


Fig. 4. Calculated K and L convergence.

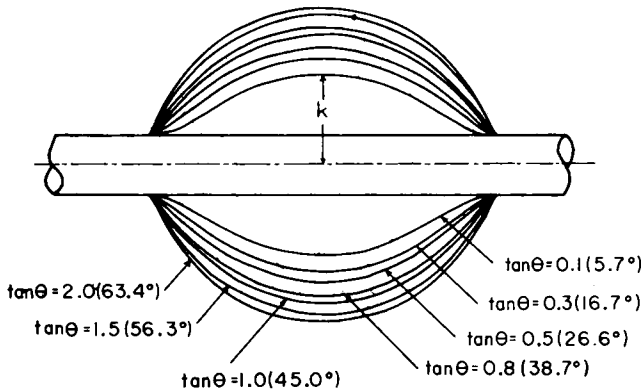


Fig. 5. Variation of drop shape with the same L -changing contact angle.

cating roughness of approximate calculation. Numerical result convergences are shown in Figure 4 under conditions $d = 2$, $\tan \theta = 0.1$, and $\Delta P = 0.5 \gamma_{LV}$. No differences exist among the results from $\Delta x = 0.1, 0.01, 0.001$, so calculations within $\Delta x \leq 0.1$ gives correct results.

If three parameters l , k , and d are measured with the use of a microscope, contact angle can be obtained from eqs. (10) and (11) and Figure 3.

Drop-shape variation is shown in Figure 5 with the same L -changing contact angle. K changes greatly with contact-angle variation.

The L -, α -Method

Contact angle can not be measured directly because of the steep liquid surface change, but apparent contact angle (α) at which the liquid surface curve becomes linear ($d^2y/dx^2 = 0$) can be measured easily. The second method is to obtain θ from L and α . The relations between θ and (L, α) are calculated from eqs. (4), (5), and (6) and are shown in Figure 6. Numerical result convergence is shown in Figure 7 under conditions $d = 2$, $\tan \theta = 0.1$, and $\Delta P =$

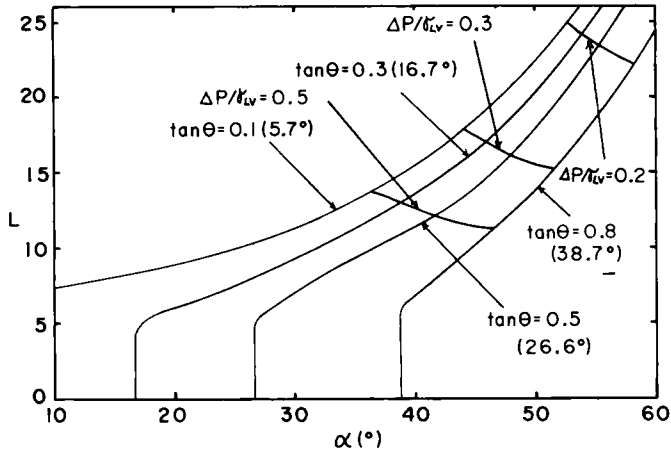


Fig. 6. Calculated relations between L and α under conditions of contact angles (θ) = 5.7°, 16.7°, 26.6°, and 38.7°.

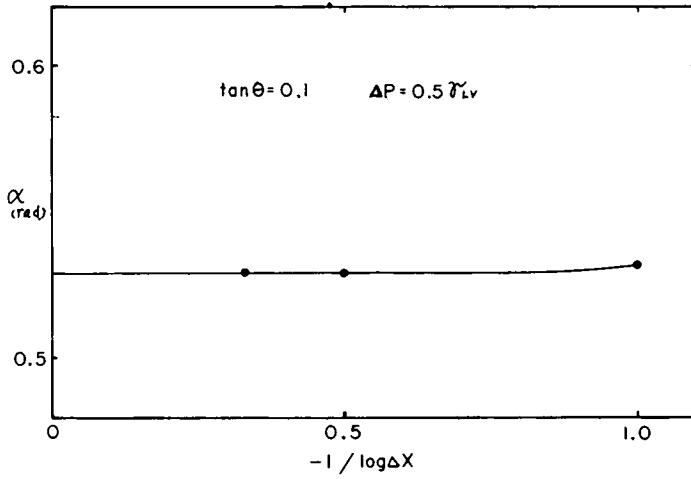


Fig. 7. Calculated α convergence.

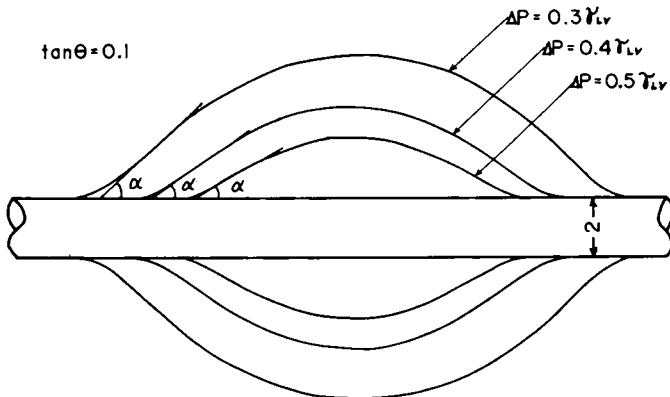


Fig. 8. Drop-shape variation with various ΔP values and fixed θ .

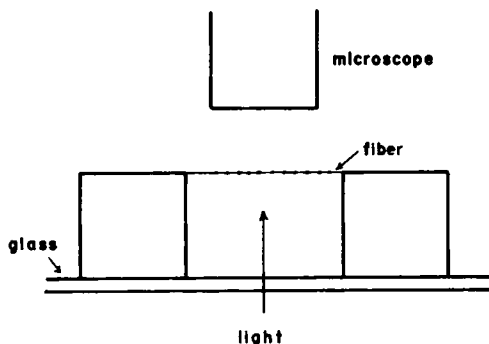


Fig. 9. Experimental method.

$0.5\gamma_{LV}$. No α difference can be found between $\Delta x = 0.01$ and 0.001 , so calculation within $\Delta x \leq 0.01$ gives a correct result.

The contact angle can be obtained from eq. (10) and Figure 6 with the use of microscopically measured parameters d , l , and α .

The difference in α is shown in Figure 8 with various $\Delta P/\gamma_{LV}$ and fixed θ . Drop volume increases with increase of apparent contact angle (α).

The K-, α -Method

This method is similar to the L -, α -method. The difference is only the use of K instead of L . However, K and α do not vary largely with variation of $\theta - \Delta P/\gamma_{LV}$, so the method is not detailed in this paper.

EXPERIMENTAL

Experimental Method

Photographs of epoxy resin (Shell Chemical Co. Epikote 828) drops attached to various kinds of monofilaments were taken by using a microscope with a camera, as shown in Figure 9. Measurement was done in a constant-temperature room at 20°C . Two rests were put on a glass plate, and a monofilament was laid between the rests. Photographs were taken from above. Care was taken that the monofilament was at right angles to the microscope.

A monofilament dipped in liquid epoxy resin was pulled out into the air. After a while, the epoxy resin attached to the monofilament formed drops. Consequently, the measured contact angle is a receding contact angle.

Comparison Between Theory and Experiment

Photomicrographs ($\times 150$) of epoxy resin drops attached to glass fiber are shown in Figure 10, and theoretical shapes of drops are shown in Figure 11. Theoretical shapes were calculated under conditions $\tan \theta = 0.1$, and K which was obtained from the photographs. Theoretical shapes were found to be completely consistent with the photographs.

Various sizes of epoxy resin were attached to untreated carbon fiber (Nippon Carbon Co., Ltd, Carbolon Z-2). Cross-sectional shape of the carbon

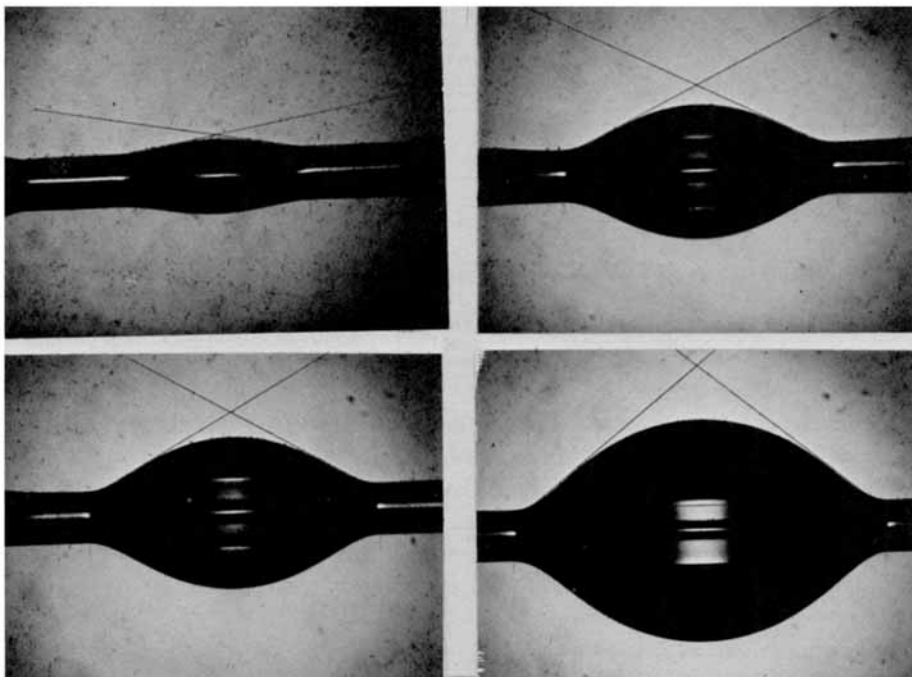


Fig. 10. Photomicrograph of epoxy resin drops attached to glass fiber ($\times 150$).

fiber is shown in Figure 12. It was found that the carbon fiber formed a cylinder, so the theory was acceptable.

Values (K, L) and (L, α) measured through use of photomicrographs ($\times 600$) are shown in Figures 13 and 14. It was found that the measured values coincided with theoretical curves.

Contact-Angle-Measurement Examples

Contact angles between epoxy resin and various monofilaments; namely, polyethylene, polycarbonate, nylon 6, poly(vinyl chloride), acetal copolymer, and glass, were measured. Results are shown in Figures 15 and 16.

In order to prepare glass fibers, a glass rod was melted with a gas burner

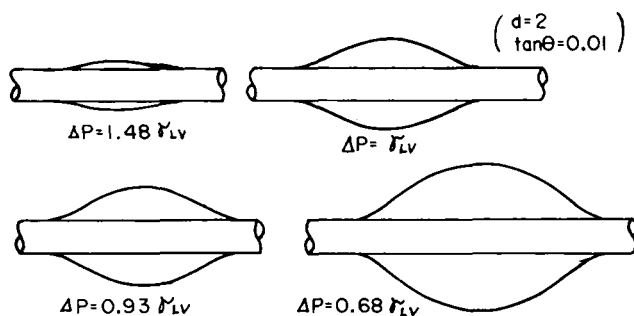


Fig. 11. Theoretical shapes of drops under conditions of $\tan \theta = 0.1$, and K which coincides with photographs.

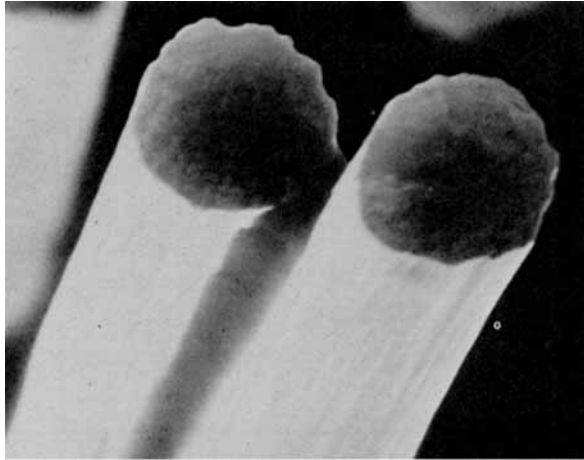


Fig. 12. Photomicrograph of carbon fiber cross-sectional shape.

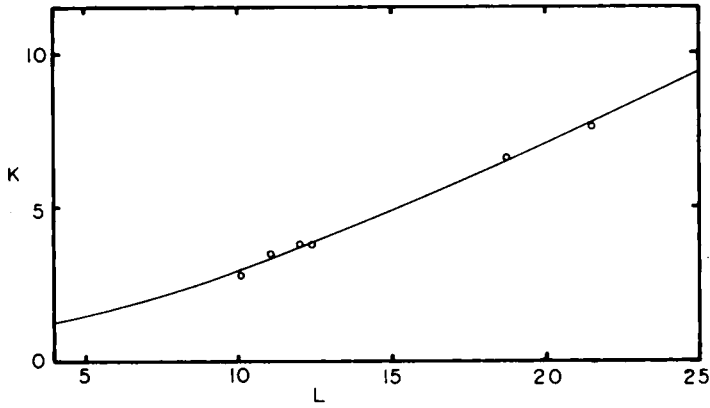


Fig. 13. Comparison with experiments, L -, K -method: \circ = measured L , K of carbon fiber/epoxy resin, with use of photomicrograph ($\times 600$); — = theoretical curve with $\theta = 17^\circ$.

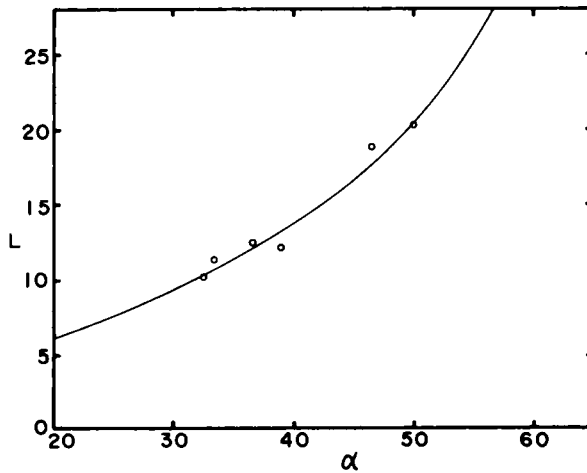


Fig. 14. Comparison with experiments, L -, α -method: \circ = measured L , α of carbon fiber/epoxy resin, with use of photomicrographs ($\times 600$); — = theoretical curve with $\theta = 17^\circ$.

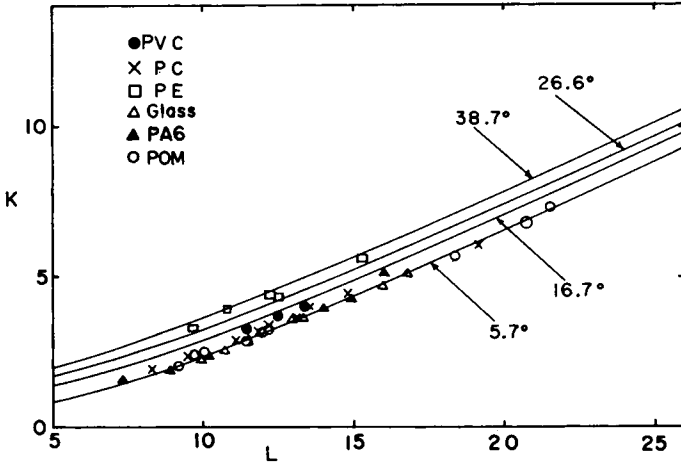


Fig. 15. Examples of contact-angle measurement, L -, K -method.

and pulled. Polyethylene fibers were also made by means of the same method as that used to form glass fibers. A flow tester was used to prepare other kinds of fibers. Molten polymers were pulled through a nozzle forming fine fibers.

Parameters (K, L, α) were measured from photomicrographs ($\times 150$). As shown in Figures 15 and 16, differences in contact angle were found among polyethylene, poly(vinyl chloride), polycarbonate, and acetal copolymer. However, it was difficult to see differences among glass, nylon 6, and acetal copolymer. This tendency is clearly shown in Figure 15 (the K -, L -method).

The contact angles obtained from both the K -, L - and L -, α -methods are shown in Table I. Comparison of these two methods shows that values from the L -, α -method were somewhat smaller than that those from the K -, L -method, except in the case of polyethylene fiber, but that differences were within experimental error. Deviations in L -, α -method experimental data

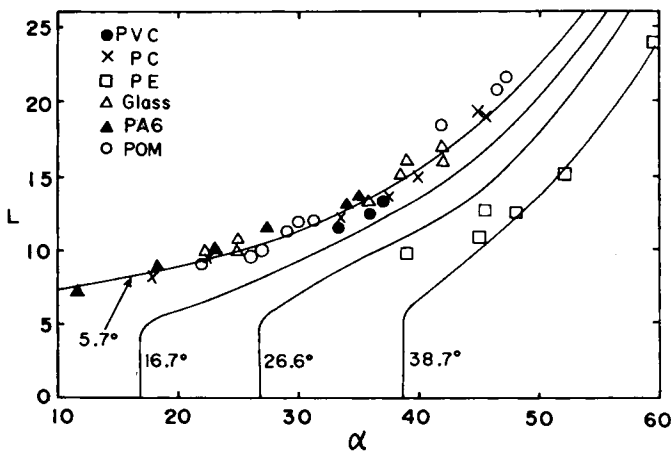


Fig. 16. Examples of contact-angle measurement, L -, α -method.

TABLE I
Epoxy Resin Contact Angle on Various Monofilaments, 20°C

| Fiber | Contact angle <i>L</i> -, <i>K</i> -method | Contact angle, <i>L</i> -, α -method |
|----------------------|---|--|
| Carbon | 17° | 17° |
| Polyethylene | 33° | 34° |
| Poly(vinyl chloride) | 13° | 12° |
| Polycarbonate | 10° | 9° |
| Nylon 6 | 6° | 5° |
| Glass | 6° | 5° |
| Acetal copolymer | 6° | 5° |

TABLE II
Contact Angle Between Epoxy Resin and Carbon Fiber

| Epoxy resin | Carbon fiber | Contact angle | Reference no. |
|----------------|---------------|---------------|------------------|
| ERLA-0400 | Thornel 25 | 12 ± 7° | 3 |
| ERL-2774 | Thornel 25 | 32 ± 8° | 3 |
| Araldite MY750 | Thermolon S-M | 72° | 2 |
| Araldite MY750 | Thermolon S-T | 69° | 2 |
| Epikote 828 | Carbolon Z-2 | 17° | authors |

TABLE III
Estimated Contact Angle Between Epoxy Resin and Polymer

| Polymer | Cosine of the contact angle (authors') | | Critical surface tension, dyn/cm | Cosine of the contact angle, (estimated) | Reference no. |
|----------------------|---|------------------------------|---|--|------------------|
| | <i>L</i> -, <i>K</i> -method | <i>L</i> -, α -method | | | |
| Polyethylene | 0.84 | 0.84 | 31 | 0.6 ~ 0.8 | 5 |
| | | | 28 | | 6 |
| Poly(vinyl chloride) | 0.97 | 0.98 | 39 | 0.85 ~ 1.0 | 7 |
| Nylon 6 | 0.99 | 1.00 | 42 | ~1.0 | 5 |

were larger than deviations in the *K*-, *L*-method, because α -experimental errors were large. With respect to polyethylene fiber: as the deviations of measured parameters were rather large, the obtained contact angle does not seem to be reliable.

The contact angles^{2,3} between epoxy resin and carbon fiber measured with the usual direct method were compared with our datum (see Table II). Our datum of contact angle seems to be compatible with the data of Bobka and Lowell (ref. 3). The data of Yamamoto et al. (ref. 2) may be overestimated, because direct measurement of the contact angle is very difficult.

The graph of $\cos \theta$ versus γ_{LV} is generally a straight line. So the contact angles of polyethylene, poly(vinyl chloride), and nylon 6 were estimated by using the $\cos \theta$ - γ_{LV} relation,^{5,6,7} where surface tension of the epoxy resin was 45 dyn/cm. The results were shown in Table III. It was found that our contact angles were not so different from the estimated contact angles.

CONCLUSIONS

First, differences between drops attached to a monofilament and those on a plate were made clear. If the drop is very small, the effect of gravity is negligible. Such small drops on a plate have similar spherical surfaces independent of liquid volume, so that the contact-angle-measurement error is small. On the contrary, it was found theoretically and experimentally that the shapes of drops attached to monofilaments changed depending on liquid volume. Moreover, the liquid surface slope changed steeply near the point where liquid surface contacted the monofilament. Accordingly, there is large experimental error in direct measurement of the contact angle between liquid and monofilament.

The reason these differences appear can be considered to be as follows: The circle that is a boundary between the liquid surface and the plate becomes larger as liquid volume increases, but the boundary between the liquid surface and the monofilament does not become larger and maintains the monofilament circumference.

Second, the practical possibility of determining a drop-shape method for measuring contact angles with monofilaments, instead of by using the ordinary direct measurement, was studied. Theoretical curves for contact-angle determination can be used, even if the liquid is not the epoxy resin used in this study, because the parameters of curves are the ratio of pressure difference to surface tension between liquid and gaseous phases $\Delta P/\gamma_{LV}$.

Third, in order to improve measurement accuracy, it is desirable to investigate some factors, for instance, improvement of microscopic resolving power and use of other drop-shape parameters, drop volumes, etc.

APPENDIX

Gravity-Neglect Approximation

When eq. (4) was derived, gravity was assumed to be negligible. The assumption is proper for the following reason.

The change of pressure difference ΔP caused by gravity is less than $2\rho gk$ where ρ is liquid density and g is gravity acceleration. Therefore, if $2\rho gk$ is negligible compared with ΔP , the approximation is approved.

Relations between ΔP and K are shown in Figure 3. In this case, the monofilament diameter is 2. The difference between ΔP and $2\rho gk$ becomes smallest in Figure 5 in the case of $\Delta P = 0.2 \gamma_{LV}$, $K = 9.5$, $\tan \theta = 2$. Now, assuming $\gamma_{LV} > 20$ dyn/cm, $\rho = 0.5$ g/cm³, and $d = 10\mu$, then ΔP and $2\rho gk$ are calculated as follows: The dimension of $\Delta P/\gamma_{LV}$ is $1/\mu$ if d is measured with the dimension of μ . We can find a similar drop whose pressure difference (ΔP) is n times the original one when monofilament diameter becomes one- n th, as mentioned in a previous section. (See "Appearance of Similar Drops.") So

$$\Delta P > 0.20(1/\mu) \times (1/5) \times 20(\text{dyn/cm}) = 0.8 \times 10^4 \text{dyn/cm}^2 \quad (\text{A-1})$$

$$2\rho gk = 2 \times 0.5 \times 980(\text{dyn/cm}^3) \times 9.5 \times 5(\mu) = 4.7 \text{dyn/cm}^2 \quad (\text{A-2})$$

Then

$$\Delta P + 2\rho gk = \Delta P. \quad (\text{A-3})$$

References

1. W. A. Zisman, in *Contact Angle, Wettability and Adhesion*, Advances in Chemistry Series, No. 43, R. F. Gould, Ed., Amer. Chem. Soc., Washington, D. C., 1964, p. 2.
2. M. Yamamoto, S. Yamada, Y. Sakatani, M. Taguchi, and Y. Yamaguchi, International Conference on Carbon Fibres, Their Composites and Applications, No. 21, London, 1971.
3. R. J. Bobka and L. P. Lowell, *AFML-TR-66-310, Pt. I*, Air Force Materials Laboratory, Dayton, Ohio, October 1966, p. 145.
4. P. Laplace, *Méchanique Céleste*, Suppl. to Vol. 10, 1806, quoted in *Encyclopedia Britanica*, Vol. 21, p. 594.
5. H. W. Fox and W. A. Zisman, *J. Colloid Sci.*, **7**, 428 (1952).
6. E. Wolfram, *Kolloid-Z.*, **182**, 75 (1962).
7. A. H. Ellison, H. W. Fox, and W. A. Zisman, *J. Phys. Chem.*, **57**, 622 (1953).

Received July 11, 1974

Revised March 17, 1975